Macromolecules
ARTICLE

Macromolecules **2009**, *42*, 9275–9288 **9275**
DOI: 10.1021/ma900930q

Synthesis and Characterizations of Highly Fluorinated Poly(arylene ether)s for Quadratic Nonlinear Optics

Khaled Aljoumaa,[†] Yinghua Qi,[‡] Jianfu Ding,[‡] and Jacques A. Delaire*,[†]

[†]*Photophysique et Photochimie Supramoléculaires et Macromoleculaires, Institut d'Alembert, Ecole Normale Supérieure de Cachan, CNRS, 61 avenue du Président Wilson, 94235 Cachan Cedex, France and* [‡]*Institute for Chemical Process and Environmental Technology, National Research Council of Canada, 1200 Montreal Road, Ottawa, Ontario, Canada K1A 0R6*

Received April 28, 2009; Revised Manuscript Received October 22, 2009

ABSTRACT: New highly fluorinated poly(arylene ether sulfone)s (FPAES), poly(arylene ether ketone)s (FPAEK), and poly(arylene ether)s with several types of NLO chromophores as pendant groups were obtained by a polycondensation reaction using very mild conditions. The different polymer structures were designed with the objective to investigate the influence of both the polarity of the chromophore and the nature of the tether between the NLO chromophore and the chain. The resulting copolymers have glass transition temperatures (T_g's) varying between 160 and 215 °C, and they are stable up to 280 °C under nitrogen. Although these copolymers are soluble in common organic solvents, cyclohexanone gave the best film quality and was used for the film preparation. After optimization of the poling conditions, the in situ second harmonic generation (SHG) measurements gave nonresonant values of the second-order susceptibilities d_{33} ranging from 2 to 8 pm/V, and the SHG signals of the poled polymer films were found to be thermally stable below 130 °C. Although being comparable with the values obtained for similar polymers and chromophores in the literature, d_{33} are smaller than those obtained for more conventional NLO polymers like PMMA−Disperse Red One (PMMA-DR1), which was taken as a reference. An unusual drop of the SHG signal during cooling was found in the thermally assisted orientation process. This drop occurred at a characteristic temperature below T_g. In this relaxation process which has never been observed, intra- and interchain dipolar interactions are shown to play an important role, which is amplified in the case of chromophores which have their donor group embedded in the main chain, connected by two rigid tethers.

Introduction

During the past two decades, organic nonlinear optical (NLO) polymers have received a considerable interest because of their potential applications in optical telecommunication devices.[1,2] Compared to inorganic crystals generally used for the manufacture of these devices, organic polymers present several advantages such as a large nonresonant optical nonlinearity of pure electronic origin, a very high bandwidth associated with a low dielectric constant, and easy processing methods for the manufacture of integrated optical devices. Furthermore, molecular engineering enables to vary the polymeric structures in order to fulfill a large variety of requirements necessary for device fabrication and practical use in terms of efficiency and long-term stability.

One of the major problems with second-order NLO polymers, for which the main target application is the manufacture of electro-optic modulators, is the long-term relaxation of the dipole orientation generally induced by a thermally assisted electric field poling and necessary to induce the non-centrosymmetry required for second-order NLO properties.[3] Different approaches have been used: first, cross-linking polymers during or after poling has been extensively investigated in recent years and has been shown to lead to an increased thermal stability.[4−7] As cross-linking often leads to increased optical losses, new 3-dimensional NLO polymeric or dendrimeric systems have been recently proposed.[8] Second, the use of polymers with a rigid polymer backbone exhibiting a high glass transition temperature (T_g) also leads to a much better thermal stability of the NLO response and has impulsed the development of new families of thermostable NLO polymers like polyimides,[9−19] polyurethanes,[20−27] polycarbonates,[28] polyquinolines,[29] and polyquinoxalines.[30]

Another important issue is the control of dipolar interactions. Because highly efficient NLO polymers bear highly dipolar chromophores with a large dipole moment, it is difficult to achieve efficient electro-optic activity due to the strong dipole−dipole interaction between the chromophores. Different strategies are being explored for improving the poling efficiency, including the use of dendronized NLO chromophores and polymers[31] and the intercalation of bulky spacers alternating with NLO chromophores along the polymer chain.[32]

As most of the NLO devices will work at the telecommunication optical bands at 1.31 and 1.55 μm, optical transparency in this wavelength range is also a critical issue. Hydrocarbon-based polymers have overtone absorptions associated with the C−H vibrations around 1500 nm, which can be responsible for significant optical loss.[33−37] In order to reduce these losses, a wide range of fluorinated polymers have been proposed, as replacing C−H bonds by C−F bonds largely reduce the overtone absorption. First developed for the manufacture of passive optical waveguides, these polymers include polyesters,[38−42] polyethers,[43−47] and polyimides.[48] Second- and third-order NLO-active fluorinated polymers have also been synthesized and characterized; they have exhibited good efficiency and thermal stability.[49−52]

In this paper, we describe the synthesis and characterization of 10 new highly fluorinated poly(arylene ether)s functionalized with different NLO chromophores (see Scheme 1). Some of us have already developed a range of highly fluorinated

*To whom correspondence should be addressed.

Published on Web 11/09/2009

Scheme 1. Chemical Structures of the Copolymers Prepared for This Paper[a]

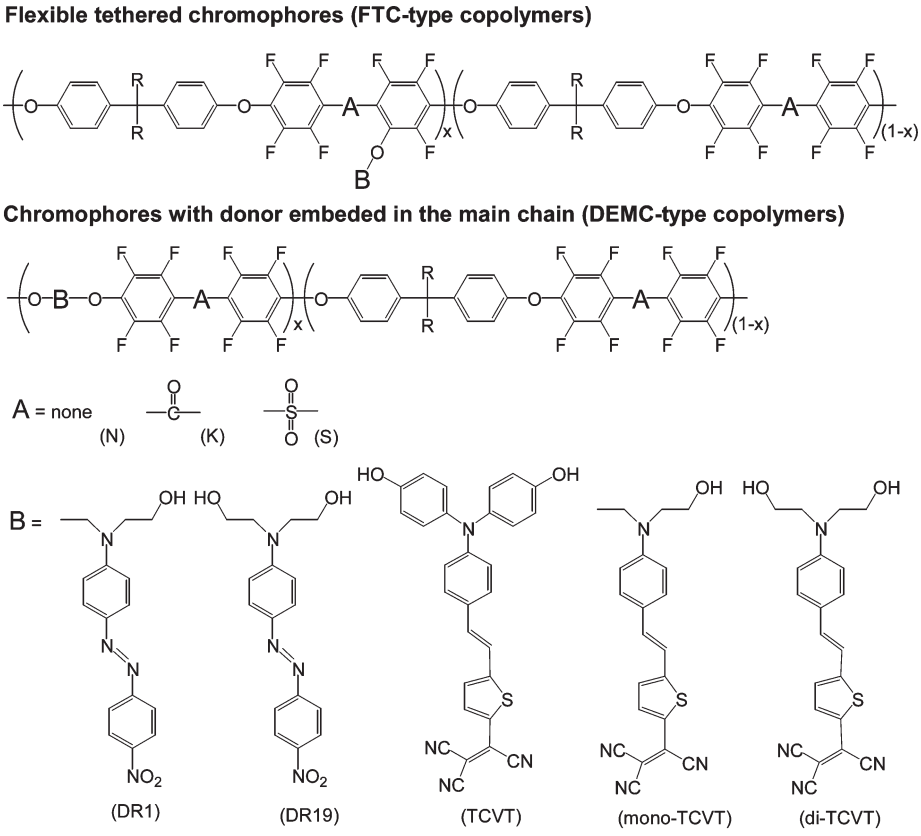

Copolymer	Chromophore linkage	R	x	A	B
FPAES-DR19-3	DEMC	CF_3	0.25	S	DR19
FPAES-DR19-5	DEMC	CF_3	0.50	S	DR19
FPAES-TCVT-1	DEMC	CF_3	0.14	S	TCVT
FPAES-TCVT-3	DEMC	CF_3	0.33	S	TCVT
FPAEK-TCVT-1	DEMC	CF_3	0.14	K	TCVT
FPAEK-TCVT-3	DEMC	CF_3	0.33	K	TCVT
PBA-TCVT-2	DEMC	CH_3	0.23	N	TCVT
FPAES-di-TCVT-3	DEMC	CF_3	0.33	S	TCVT
FPAES-mono-TCVT-3	FTC	CF_3	0.30	S	TCVT
FPAES-DR1-6	FTC	CF_3	0.64	S	DR1

[a] The monomer structure of B units was displayed for easy understanding the polymer synthesis. They were incorporated into the polymers through the OH groups.

poly(arylene ether sulfone)s (FPAES) and poly(arylene ether ketone)s (FPAEK) for optical waveguide applications.[53−58] A new efficient synthetic method has been developed for their preparation with high molecular weight and linear structures[53] and the incorporation of cross-linkable groups inducing a reduced birefringence.[55] FPAES and FPAEK represent a series of promising materials that enable the balance of properties such as birefringence, glass-transition temperature, and adhesion by adjusting the structure and fluorine content. In order to make these polymers active in NLO, different chromophores with large first hyperpolarizability coefficients have been incorporated into or on the polymer backbone. These new NLO copolymers should fulfill several requirements, like high T_g and low optical losses around 1.5 μm. In order to investigate the effect of the backbone flexibility and the linkage structure on the performance of nonlinear optical polymers, TCVT chromophore containing tricyanovinylthiophene acceptor and aminophenyl donor has been introduced into FPAES and FPAEK as a pendent side group through three different manners as illustrated in Scheme 1, i.e., DEMC (chromophore with donor embedded in the main chain) type with phenylene linkages, DEMC type with ethylene linkages, and FTC (flexible tethered chromophores) type. On the other hand, another type of chromophore, Disperse Red (DR19 and DR1), was also introduced into the polymers to compare the effect of the chromophore polarity.

The second-order NLO coefficients of these polymers and their thermal stability have been determined by in situ second harmonic generation (SHG). They have been compared and discussed in comparison with a standard NLO polymer, PMMA-DR1. One preliminary report concerning four of these polymers has already been published.[59]

Experimental Section

Materials. The solvents used for polymerization and for sample processing including anhydrous *N*,*N*-dimethylacetamide and cyclohexanone are analytical reagent and used as

received. A reference NLO polymer, PMMA-DR1, is a gift from Alain Rousseau (Ecole Nationale Supérieure de Chimie de Montpellier) containing 24 mol % chromophore, and the characterization data can be found in the literature.[60] The following chromophore precursors were synthesized following the cited literature procedures: (*E*)-4,4′-(4-(2-(thiophen-2-yl)vinyl)phenylazanediyl)diphenol (ThV),[20] (*E*)-2,2′-(4-(2-(thiophen-2-yl)vinyl)phenylazanediyl)diethanol (di-ThV),[20] and (*E*)-2-(ethyl(4-(2-(thiophen-2-yl)vinyl) phenyl) amino)ethanol (mono-ThV).[20] Fluorinated poly(arylene ether sulfone), FPAES, and poly(arylene ether ketone), FPAEK, have been prepared using a similar process as reported previously,[55c] and their characterization data are summarized in Table 1.

Synthesis of the Model Compound TCVT (See Scheme 2). ThV (0.77 g, 2.0 mmol) and tetracyanoethylene, TCNE (1.04 g, 8.0 mmol) were added into a 15 mL vial; the system was evacuated and filled with argon. 8.0 mL of *N,N*-dimethylformamide (DMF) (freshly distilled over CaH_2) was added into the vial under stirring, and the mixture was stirred at 40 °C under the protection of argon for 36 h. The solution was dropped into 100 mL of water to precipitate the product as a dark blue powder. It was dried and further purified by column chromatography using chloroform as eluent to give TCVT (0.53 g, 54% yield). ^{1}H NMR (400 MHz, acetone-d_6) δ (ppm): 8.42 (s, ∼1H), 8.09 (d, J = 4.2 Hz, 1H), 7.53 (d, J = 8.8 Hz, 2H), 7.52 (d, J = 4.2 Hz, 1H), 7.52 (d, J = 16.4 Hz, 1H), 7.43 (d, J = 16.4 Hz, 1H), 7.07 (d, J = 8.8 Hz, 4H), 6.87 (d, J = 8.8 Hz, 4H), 6.77 (d, J = 8.8 Hz, 2H).

General Procedure for the Preparation of DEMC-Type ThV or DR19 Copolymers Listed in Scheme 3. One of the decafluorodiphenyl compounds (1.01 equiv of decafluorodiphenylsulfone, DFPSO, decafluorobenzophenone, DFBP, or decafluorobiphenyl, DFP), hexafluorobisphenol-A (6F-BPA) or bisphenol A (BPA) ((1 − x) equiv), chromophore diol or bisphenol (x equiv), and cesium fluoride (CsF, 3.0 equiv) were introduced into a flask with a stir bar. The flask was closed, evacuated, and filled with argon. Anhydrous DMAc was added to form a solution at a solid concentration of 5−10%. The reaction mixture was stirred at room temperature for 6−12 h and then centrifuged. The supernatant was precipitated into methanol, and the resulting fiber-like powder was collected by filtration and washed twice with methanol and dried under vacuum for 12 h to yield the desired polymer.

FPAES-DR19-3. Prepared from DFPSO (0.8004 g, 2.01 mmol), 6F-BPA (0.5043 g, 1.50 mmol), and DR19 (0.1651 g, 0.50 mmol) to yield 1.25 g of red fiber-like powder (yield: 90%). ^{1}H NMR (400 MHz, THF-d_8): δ (ppm) 8.32 (d, J = 8.4 Hz, 2H), 7.94 (d, J = 8.2 Hz, 2H), 7.88 (d, J = 8.2 Hz, 2H), 7.41 (m, 12H), 7.14 (m, 12H), 7.00 (m, 2H), 4.76 (m, 4H), 4.14 (m, 4H). ^{19}F NMR (376 MHz, DMSO-d_6): δ (ppm) −63.8 (18F, CF_3), −136.5, −136.9, −138.1, −138.5 (d, J = 15.8 Hz, ortho-F, 16F in total with ratio = 9:3:3:1), −151.1, −151.3, −155.3, −155.5 (meta-F, 16F in total with ratio = 9:3:3:1). M_n: 50.6 kDa; M_w/M_n: 4.6; T_g: 178 °C; $T_d^{1\%}$: 285 °C.

FPAES-DR19-5. Prepared from DFPSO (0.8004 g, 2.01 mmol), 6F-BPA (0.3362 g, 1.00 mmol), and DR19 (0.3303 g, 1.00 mmol) to yield 1.22 g of deep red fiber-like powder (yield: 88%). ^{1}H NMR (400 MHz, THF-d_8): δ (ppm) 8.30 (d, J = 8.4 Hz, 2H), 7.92 (d, J = 8.4 Hz, 2H), 7.85 (d, J = 8.4 Hz, 2H), 7.40 (m, 4H), 7.18 (m, 4H), 6.99 (m, 2H), 4.73 (m, 4H), 4.12 (m, 4H). ^{19}F NMR (376 MHz, DMSO-d_6): δ (ppm) −63.8 (6F, CF_3), −136.9, −137.3, −138.5, −138.8 (d, J = 15.8 Hz, ortho-F, 8F in total with ratio = 2:2:2:2) −151.6 (m, 4F), −155.8 (m, 2F). M_n: 38.0 kDa; M_w/M_n: 2.5; T_g: 171 °C; $T_d^{1\%}$: 264 °C.

FPAES-ThV-1. Prepared from DFPSO (0.565 g, 1.42 mmol), 6F-BPA (0.403 g, 1.20 mmol), and ThV (0.077 g, 0.20 mmol) to yield pale yellow fiber-like powder. ^{1}H NMR (400 MHz, acetone-d_6): δ (ppm) 7.51−7.42 (m, 26H), 7.37−7.27 (m, 26H), 7.18 (d, J = 8.2 Hz, 4H) 7.14−7.09 (m, 5H), 7.01 (dd, J = 2.8 Hz, 1H), 6.98 (d, J = 8.4 Hz, 2H), 6.93 (d, J = 16.4 Hz, 1H).

Table 1. Characterization of Synthesized Copolymers

		TCVT polymer				ThV polymer							
copolymers	chrom loading (mol %)	M_n (g/mol)	PDI	T_g (°C)[a]	T_d (°C)[b] 1% (5%)	M_n (g/mol)	PDI	T_g (°C)[a]	T_d (°C)[b] 1% (5%)	roughness (nm) ± 0.1 nm	$n_{1907\pm0.01}$	$n_{954\pm0.01}$	λ_{max} for film (λ_{max} in cyclohexanone) (nm) (±2)
homo-FPAEK		25 000	3.2	151	415 (446)								
homo-FPAES		72 800	3.5	182	430 (473)								
FPAES-DR19-3	25	50 600	4.6	178	285 (288)					0.4	1.54	1.56	445 (462)
FPAES-DR19-5	50	38 000	2.5	171	264 (266)					0.6	1.57	1.59	445 (462)
FPAES-DR1-6	64	40 800	17.5	174	286 (310)					2.2	1.52	1.55	480 (480)
FPAES-mono-TCVT-3	30	36 600	10.1	195	277 (320)	380 000	11.3	171	262 (301)	2.5	1.53	1.57	615 (612)
FPAES-di-TCVT-3	33	13 900	8.8	185	271 (284)	20 800	8.7	164	266 (274)	2.0			623 (615)
FPAES-TCVT-1	14	19 300	6.9	196	352 (434)	36 400	2.8	171	447 (484)	0.6	1.53	1.56	618 (614)
FPAES-TCVT-3	33	19 700	7.5	213	380 (454)	25 900	3.4	195	422 (462)	0.4	1.61	1.67	618 (612)
FPAEK-TCVT-1	14	20 700	9.9	168	364 (486)	30 900	5.1	154	448 (486)	0.7	1.52	1.55	621 (617)
FPAEK-TCVT-3	33	46 700	9.1	187	359 (464)	28 500	5.9	159	406 (485)	0.5	1.58	1.65	621 (617)
PBA-TCVT-2	23	28 100	9.5	182	415 (477)			175		0.6	1.54	1.58	624 (618)

[a] Glass transition temperature from DSC measurement. [b] Decomposition temperature at 1% (5%) weight loss from TGA measurement.

^{19}F NMR (376 MHz, acetone-d_6): δ (ppm) −63.8 (36F, CF_3), −137.25 (24F ortho-F adjacent to BPA), −137.66 (4F, ortho-F adjacent to ThV), −151.92 (24F, meta-F adjacent to BPA), −152.50 (4F, meta-F adjacent to ThV). M_n :36.4 kDa, M_w/M_n: 2.8; T_g: 171 °C; $T_d^{1\%}$: 447 °C.

FPAES-ThV-3. Prepared from DFPSO (0.602 g, 1.52 mmol), 6F-BPA (0.336 g, 1.00 mmol), and ThV (0.193 g, 0.50 mmol) to yield pale yellow fiber-like powder. ^{1}H NMR (400 MHz, DMSO-d_6): δ (ppm) 7.44 (d, J = 8.0 Hz, 2H), 7.34 (m, 17H), 7.26 (d, J = 16.4 Hz, 1H), 7.18 (d, J = 8.4 Hz, 4H), 7.13 (m, 1H), 7.06 (d, J = 8.2 Hz, 4H), 7.01 (m, 1H), 6.89 (d, J = 8.4 Hz, 2H), 6.86 (d, J = 16.4 Hz, 1H).^{19}F NMR (376 MHz, DMF-d_6): δ −63.8 (6F, CF_3), −137.45 (4F, ortho-F adjacent to BPA), −137.86 (2F, ortho-F adjacent to ThV), −152.05 (4F, meta-F adjacent to BPA), −152.52 (6F, meta-F adjacent to ThV).

Scheme 2. Reaction Scheme for the Preparation of TCVT

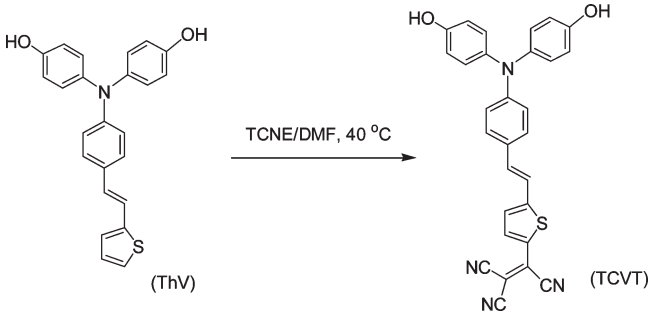

IR (cm^{-1}): 2974 w, 2873 w, 1638 m, 1605 m, 1492 vs, 1388 m, 1320 w, 1177 vs, 1097 s, 996 s, 827 w, 600 m. M_n: 25.9 kDa, M_w/M_n: 3.4, T_g: 195 °C; $T_d^{1\%}$: 422 °C.

FPAEK-ThV-1. Prepared from DFBP (0.514 g, 1.42 mmol), 6F-BPA (0.403 g, 1.20 mmol), and ThV (0.077 g, 0.20 mmol) to yield pale yellow fiber-like powder. ^{1}H NMR (400 MHz, acetone-d_6): δ (ppm) 7.52−7.42 (m, 26H), 7.37−7.26 (m, 26H), 7.22−7.06 (m, 8H), 7.04−6.94. (m, 4H), 6.92 (d, J = 16.4 Hz, 1H). ^{19}F NMR (376 MHz, acetone-d_6): δ (ppm) −63.8 (36F, CF_3), −142.3, −142.4, −142.6, −142.7 (ortho-F, 28F in total, ratio = 36:6:6:1), −153.2 (24F, meta-F adjacent to BPA), −152.6 (4F, meta-F adjacent to ThV). M_n: 30.9 kDa, M_w/M_n: 5.1; T_g: 154 °C; $T_d^{1\%}$: 448 °C.

FPAEK-ThV-3. Prepared from DFBP (0.550 g, 1.52 mmol), 6F-BPA (0.336 g, 1.00 mmol), and ThV (0.193 g, 0.50 mmol) to yield pale yellow fiber-like powder. ^{1}H NMR (400 MHz, acetone-d_6): δ (ppm) 7.52−7.41 (m, 10H), 7.37−7.25 (m, 10H), 7.21−7.07 (m, 8H), 7.04−6.93. (m, 4H), 6.92 (d, J = 16.4 Hz, 1H). ^{19}F NMR (376 MHz, acetone-d_6): δ (ppm) −63.8 (12F, CF_3), −142.3, −142.4 −142.6, −142.7 (ortho-F, 12F in total, ratio = 4:2:2:1), 2F), −153.2 (8F, meta-F adjacent to BPA), −152.6 (4F, meta-F adjacent to ThV). M_n: 28.5 kDa, M_w/M_n: 5.9, T_g: 159 °C; $T_d^{1\%}$: 406 °C.

PBA-ThV-2. Prepared from DFP (0.5350 g, 1.601 mmol), BPA (0.2603 g, 1.140 mmol), and ThV (0.1745 g, 0.453 mmol) to yield 0.75 g of pale yellow fiber-like powder (yield: 83%). ^{1}H NMR (400 MHz, acetone-d_6): δ (ppm) 7.36 (m 1H), 7.26 (d, J = 8.4 Hz, 14H), 7.19 (d, J = 8.4 Hz, 4H), 7.07 (d, J = 8.4 Hz, 17H), 7.05−6.96. (m, 2H), 6.92 (d, J = 16.4 Hz, 1H), 1.64 (m, 20H)

Scheme 3. Reaction Routes for the Preparation of the DEMC-Type ThV and DR19 Copolymers

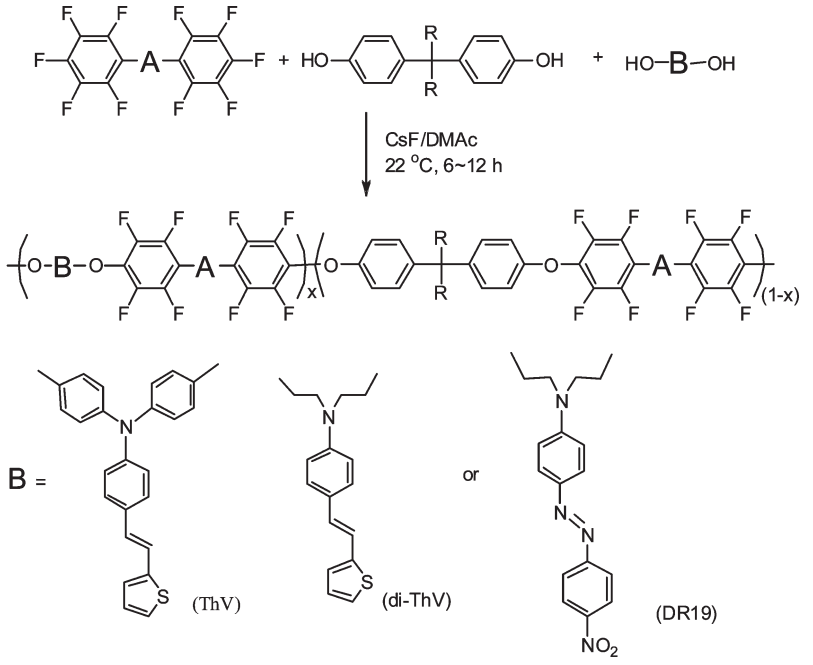

Copolymer	x	A	B	R
FPAES-DR19-3	0.25	S	DR19	CF_3
FPAES-DR19-5	0.50	S	DR19	CF_3
FPAES-ThV-1	0.10	S	ThV	CF_3
FPAES-ThV-3	0.33	S	ThV	CF_3
FPAEK-ThV-1	0.14	K	ThV	CF_3
FPAEK-ThV-3	0.30	K	ThV	CF_3
PBA-ThV-2	0.18	N	ThV	CH_3
FPAES-di-ThV-3	0.30	S	di-ThV	CF_3

Scheme 4. Chemical Reaction between ThV Polymers with TCNE in DMF at 50 °C[a]

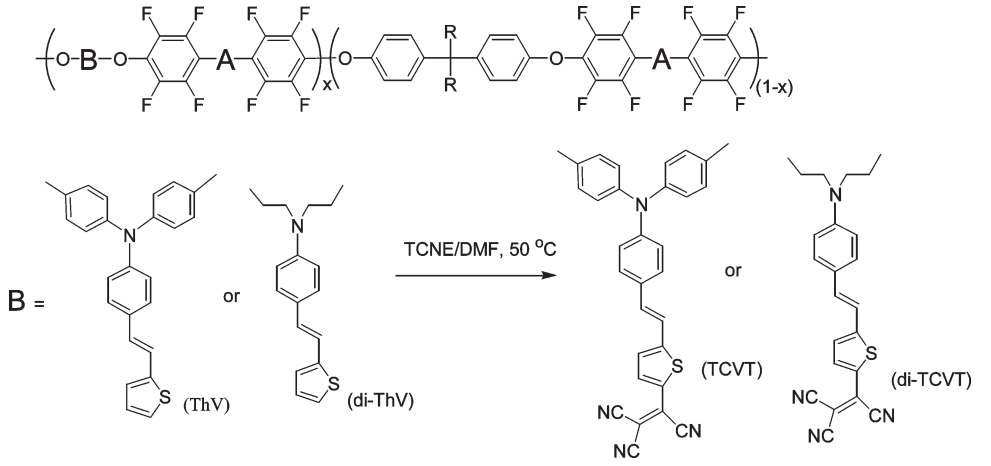

[a] Real structures of B units were displayed, while their monomer structures are in Scheme 1.

(~23% dye).[19]F NMR (376 MHz, acetone-d_6): δ (ppm) −140.42 (4F, ortho-F), −155.80 (4F, meta-F). T_g: 175 °C.

FPAES-di-ThV-3. Prepared from DFPSO (0.6022 g, 1.52 mmol), 6F-BPA (0.3362 g, 1.00 mmol), and di-ThV (0.1447 g, 0.50 mmol) to yield 0.95 g of pale yellow fiber-like powder (yield: 93%). ^{1}H NMR (400 MHz, DMSO-d_6, 50 °C): δ (ppm) 7.22−7.40 (m, 19H), 6.90−7.16 (m, 3H), 6.68−6.83 (m, 3H), 4.628 (m, 4H), 3.872 (m, 4H). ^{19}F NMR (376 MHz, DMSO-d_6, 50 °C): δ (ppm) −63.80 (9F, CF_3), −137.52, −137.89, −139.26, −139.73 (ortho-F, 12F in total, ratio = 4:2:2:1) −152.25 (8F, meta-F adjacent to BPA unit), −156.05 (4F, meta-F adjacent to di-ThV unit). IR (cm^{-1}): 2973 w, 2872 w, 1637 m, 1604 m, 1587 m, 1493 vs, 1383 m, 1223 s, 1176 vs, 1125 m, 1094 s, 995 s, 827 m, 599 s, 573 m, 557 m. M_n: 20.8 kDa, M_w/M_n: 8.7; T_g: 164 °C; $T_d^{1\%}$: 266 °C.

General Procedure for the Preparation of the TCVT Copolymers from the ThV Copolymers (See Scheme 4). ThV copolymer (1.0 equiv of thiophene group) and TCNE (6.0 equiv) were added into a vial, which was then evacuated and refilled with argon. Fresh distilled (over CaH_2) DMF was added into the vial to form a solution at ~10% polymer concentration. The solution was then placed into a 50 °C oil bath with stirring for 24 h, prior to be dropped into methanol to precipitate the product. The resulting deep blue polymer was washed with methanol for three times and then dried under vacuum for 12 h.

FPAES-TCVT-1. Prepared from FPAES-ThV-1 (0.49 g, 0.10 mmol of thiophene group) and TCNE (0.077 g, 0.6 mmol) to yield blue product. ^{1}H NMR (400 MHz, DMSO-d_6): δ (ppm) 8.03 (1H), 7.59 (1H), 7.43 (1H), 7.35 (48H), 7.23 (d, J = 8.4 Hz, 4H), 7.20−7.12 (3H), 7.06 (d, J = 8.4 Hz, 4H), 6.92−6.80 (2H). ^{19}F NMR (376 MHz, DMSO-d_6): δ (ppm) −63.8 (36F, CF_3), −137.43 (24F, ortho-F adjacent to ThV), −137.78 (4F, ortho-F adjacent to BPA), −151.95 (24F, meta-F adjacent to ThV), −152.43 (4F, ortho-F adjacent to BPA). M_n: 19.3 kDa, M_w/M_n: 6.9; T_g: 196 °C; $T_d^{1\%}$: 352 °C.

FPAES-TCVT-3. Prepared from FPAES-ThV-3 (0.4266 g, 0.20 mmol of thiophene group) and TCNE (0.154 g, 1.2 mmol) to yield deep blue product. ^{1}H NMR (400 MHz, DMSO-d_6): δ (ppm) 8.03 (1H), 7.57 (m, 3H), 7.46 (m, 1H) 7.34 (m, 17H), 7.23 (d, J = 8.2 Hz, 4H), 7.14 (d, J = 8.2 Hz, 4H), 6.86 (d, J = 8.2 Hz, 2H). ^{19}F NMR (376 MHz, DMSO-d_6): δ (ppm) −63.8 (6F, CF_3), −137.70 (4F, ortho-F adjacent to ThV), −138.11 (2F, ortho-F adjacent to BPA), −152.34 (4F, meta-F adjacent to ThV), −152.75 (2F, ortho-F adjacent to BPA). IR (cm^{-1}): 2968 w, 2871 w, 2219 w, 1637 m, 1604 m, 1587 m, 1492 vs, 1421 s, 1388 m, 1321w, 1177 vs, 1097 s, 996 s, 829 w, 600 m. M_n: 19.7 kDa, M_w/M_n: 7.5; T_g: 213 °C; $T_d^{1\%}$: 380 °C.

FPAEK-TCVT-1. Prepared from FPAEK-ThV-1 (0.47 g, 0.1 mmol of thiophene group) and TCNE (0.077 g, 0.6 mmol) to yield deep blue product. ^{1}H NMR (400 MHz, acetone-d_6): δ (ppm) 8.07 (1H), 7.64 (2H), 7.54 (1H), 7.49 (d, J = 8.4 Hz, 24H), 7.35 (d, J = 8.4 Hz, 24H), 7.23. (m, 4H), 7.22−7.10 (2H), 6.97 (d, J = 8.4 Hz, 2H), 6.92 (d, J = 16.4 Hz, 1H). ^{19}F NMR (376 MHz, acetone-d_6): δ (ppm) −63.8 (36F, CF_3), −142.4, −142.5, −142.7, −142.8, (ortho-F, 28F in total, ratio = 36:6:6:1), −153.7 (24F, meta-F adjacent to ThV), −154.1 (4F, ortho-F adjacent to BPA). M_n: 20.7 kDa, M_w/M_n: 9.9; T_g: 168 °C; $T_d^{1\%}$: 364 °C.

FPAEK-TCVT-3. Prepared from FPAES-ThV-3 (0.40 g, 0.2 mmol of thiophene group) and TCNE (0.154 g, 1.2 mmol) to yield deep blue product. ^{1}H NMR (400 MHz, acetone-d_6): δ (ppm) 8.06 (1H) 7.62 (d, J = 8.4 Hz, 2H), 7.48 (d, J = 8.4 Hz, 9H), 7.34 (d, J = 8.4 Hz, 8H), 7.23 (m, 4H), 7.22−7.10 (2H), 6.97 (d, J = 8.4 Hz, 2H), 6.92 (d, J = 16.4 Hz, 1H). ^{19}F NMR (376 MHz, acetone-d_6): δ (ppm) −63.8 (12F, CF_3), −142.59, −142.71 −142.86, −142.96 (ortho-F, 12F in total, ratio = 4:2:2:1), −153.52 (4F, meta-F adjacent to BPA), −153.91 (4F, meta-F adjacent to ThV). M_n: 46.7 kDa, M_w/M_n: 9.1; T_g: 187 °C; $T_d^{1\%}$: 359 °C.

PBA-TCVT-2. Prepared from PBA-ThV-3 (0.50 g, 0.25 mmol of thiophene group) and TCNE (0.192 g, 1.5 mmol) to yield 0.49 g of deep blue product (yield: 93%). ^{1}H NMR (400 MHz, acetone-d_6): δ (ppm) 8.03 (m, 1H), 7.59 (m, 2H), 7.58−7.44 (4H), 7.26 (d, J = 8.4 Hz, 13H), 7.20 (m, 8H), 7.07 (d, J = 8.4 Hz, 13H), 6.95 (m, 4H), 1.64 (m, 20H) (~23% dye).[19]F NMR (376 MHz, acetone-d_6): δ (ppm) −140.26 (4F, ortho-F), −155.61 (4F, meta-F). M_n: 28.1 kDa, M_w/M_n: 9.5; T_g: 182 °C; $T_d^{1\%}$: 415 °C.

FPAES-di-TCVT-3. Prepared from FPAES-di-ThV-3 (0.305 g, 0.15 mmol of thiophene group) and TCNE (0.154 g, 1.2 mmol) to yield 0.29 g of deep blue product (yield: 90%). ^{1}H NMR (400 MHz, DMSO-d_6, 50 °C): δ (ppm) 7.98 (m, 1H), 7.51 (m, 3H), 7.34 (m, 19H), 6.89 (m, 2H), 4.66 (m, 4H), 3.95 (m, 4H) ^{19}F NMR (376 MHz, DMSO-d_6, 50 °C): δ (ppm) −63.8 (9F, CF_3), −137.42, −137.95, −139.26, −139.81 (ortho-F, 12F in total, ratio = 4:2:2:1) −151.95 (8F, meta-F adjacent to BPA unit), −155.47 (4F, meta-F adjacent to di-ThV unit). IR (cm^{-1}): 2976 w, 2869 w, 2217 w, 1637 m, 1603 m, 1589 m, 1498 vs, 1423 m, 1390 m, 1359 m, 1223 s, 1175 vs, 1124 m, 1094 s, 995 s, 827 m, 814 w, 599 s, 573 m, 559 m. M_n: 13.9 kDa, M_w/M_n: 8.8; T_g: 185 °C; $T_d^{1\%}$: 271 °C.

Synthesis of FPAES-mono-TCVT-3 (FTC-Type Copolymer) (Scheme 5). FPAES (0.347 g, 0.5 mmol of repeat unit), mono-ThV (0.046 g, 0.17 mmol), and CsF (0.091 g, 0.6 mmol, dried under vacuum at 150 °C for 30 min) were added into a 10 mL vial. The vial was sealed and evacuated and filled with argon. 3 mL of anhydrous DMAc was injected into the vial. The reaction mixture was stirred at room temperature for 6 h and then was centrifuged. The supernatant was dropped into 100 mL

Scheme 5. Chemical Reaction for the Preparation of FPAES-mono-TCVT

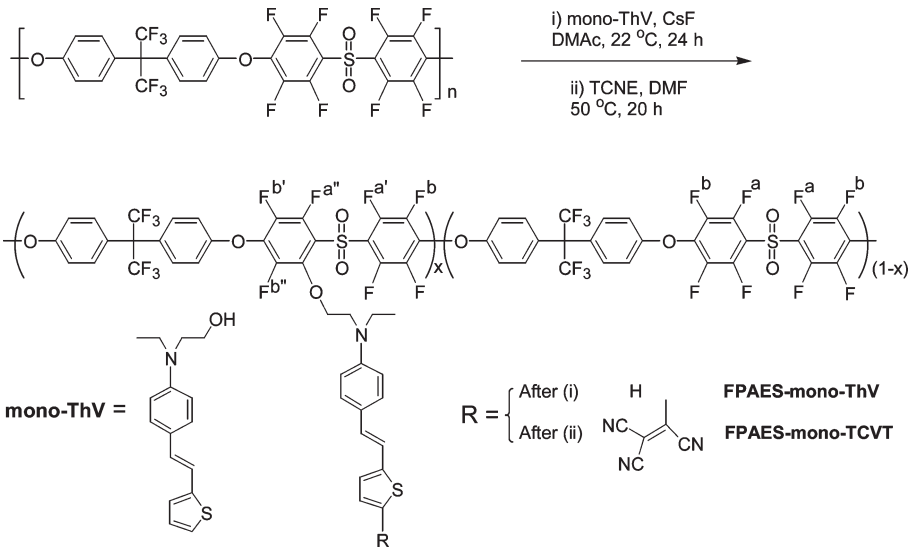

of methanol to precipitate the polymer. The resulting pale yellow powder was washed twice with methanol and dried under vacuum for 12 h to give FPAES-mono-ThV-3 with the ThV loading density of 30%. ^{1}H NMR (400 MHz, DMSO-d_6): δ (ppm) 7.20−7.40 (m, 28H), 6.90−7.14 (m, 4H), 6.60−6.82 (m, 3H), 4.28−4.65 (m, 2H), 3.62−3.80 (m, 2H), 3.26−3.48 (m, 2H), 0.95−1.15 (m, 3H). ^{19}F NMR (376 MHz, DMSO-d_6): δ (ppm) −63.8 (18F, CF_3), −137.41 (8F, a), −137.90 (2F, a′), 139.36 (1F, a″) −144.56 (1F, b′), −151.941 (10F, b), −153.47 (1F, b″). IR (cm^{-1}): 2978 w, 2871 w, 1637 m, 1605 m, 1491 vs, 1392 m, 1375 m, 1223 s, 1176 vs, 1097 s, 996 s, 968 m, 929 m, 830 m, 734 m, 601 s, 559 m. M_n: 38 000 Da. M_w/M_n: 11.3, T_g: 171 °C; $T_d^{1\%}$: 262 °C.

FPAES-mono-ThV-3 (0.234 g, 0,100 mmol) along with TCNE (0.077 g, 0.60 mmol) was then added into a 10 mL vial; the system was evacuated and filled with argon. 3.0 mL of DMF (freshly distilled over CaH_2) was added into the vial under stirring and the mixture was stirred at 50 °C under the protection of argon for 20 h. The solution was dropped into 100 mL of methanol to precipitate the polymer. The resulting blue powder was washed with methanol three times and dried under vacuum at room temperature for 12 h to give designed polymer. ^{1}H NMR (400 MHz, DMSO-d_6): δ (ppm) 7.90−8.04 (m, 1H), 7.42−7.58 (m, 2H), 7.16−7.42 (m, 28H), 6.90−7.14 (m, 1H), 6.60−6.82 (m, 2H), 4.25−4.68 (m, 2H), 3.62−3.86 (m, 2H), 3.32−3.56 (m, 2H), 0.94−1.18 (m, 3H). ^{19}F NMR (376 MHz, acetone-d_6): δ (ppm) −63.8 (18F, CF_3), −137.38 (8F, a, see Scheme 5 for assignment), −137.87 (2F, a′), −139.15 (1F, a″), −144.47 (1F, b′), −151.91 (10F, b), −153.12 (1F, b″). IR (cm^{-1}): 2978 w, 2871 w, 2218 w, 1637 m, 1605 m, 1587 m, 1504 s 1490 vs, 1420 m, 1397 m, 1223 s, 1177 vs, 1096 s, 996 s, 968 m, 929 m, 830 m, 734 m, 601 s, 559 m. M_n: 36.6 kDa, M_w/M_n: 10.1; T_g: 195 °C; $T_d^{1\%}$: 277 °C.

Synthesis of the Copolymer FPAES-DR1-6 (FTC-Type Copolymer). It was prepared by using a similar procedure for the preparation of FPAES-mono-ThV-3, by reacting FPAES (0.692 g, 1.00 mmol of DFPSO unit), with DR1 (0.3362 g, 1.00 mmol) in 5 mL of anhydrous DMAc in the presence of CsF (0.304 g, 2.00 mmol) (see Scheme 1). The reaction resulted in 0.79 g of deep red powder with the DR-1 loading density of 64% (yield: 92%). ^{1}H NMR (400 MHz, acetone-d_6): δ (ppm) 8.30 (m, 2H) 7.93 (m, 2H), 7.82 (m, 2H), 7.42 (d, J = 8.4 Hz, 6H), 7.29 (d, J = 8.4 Hz, 6H), 6.95 (m, 2H), 4.53 (m, 2H), 3.97 (m, 2H), 3.58 (m, 2H), 1.19 (m, 3H) . ^{19}F NMR (376 MHz, acetone-d_6): δ (ppm) −63.8 (18F, CF_3), −137.31 (5F), −137.89 (4F), −138.80 (2F), −144.41 (2F), −151.96 (10F), −152.82 (2F). M_n: 40.8 kDa, M_w/M_n: 17.5; T_g: 174 °C; $T_d^{1\%}$: 286 °C.

Characterization Methods. Size exclusion chromatography (SEC) spectra were collected using a Viscotek SEC system, which consists of a Viscotek VE1122 HPLC pump coupled with a Viscotek TDA triple detector and a Viscotek 2501 UV detector operated at 260 nm. A set of ViscoGEL columns (G300H, G4000H, and G5000H) was used and calibrated by a set of polystyrene standards in THF. The flow rate was 1 mL/min. The columns and the detectors were operated at 35 °C. NMR spectra were recorded using a Varian Unity Inova spectrometer (400 MHz). Thermal stability and thermodynamic transitions (glass transition) of the polymers were measured on a TA Instrument DSC 2920 and a TGA 2950 at a heating rate of 10 °C/min under nitrogen.

Thin Film Preparation and Electric Field Poling. Solutions of the fluorinated copolymers (6% w/w) in cyclohexanone were first filtered through 0.45 μm Teflon membrane filters and then spin-coated at a speed of 500 rpm onto clean glass slides. The resulting films were then vacuum-dried at 70 °C for 2 h and at 150 °C for 1 h. They were then stored in a closed box, in the dark prior to electric poling. Surface roughness of the films was examined by AFM (AFM Explorer microscope model 4400-11 from Veeco). A corona poling stage using a corona discharge with a tip to plane distance of 1 cm and a voltage of 5 kV was used to pole the films at different temperatures. This stage was fixed in an oven positioned over a rotating plate with optical windows allowing to perform second harmonic generation (SHG) measurements during and after the poling (in situ poling).

Linear and Nonlinear Optical Experimental Methods. The UV−vis absorption spectra of different copolymer films were performed on a Varian Cary 500E spectrophotometer. The spectra of refractive indices were performed by ellipsometric spectroscopy with a rotating polarizer (model SOPRA GESP5) on films deposited on silicon wafers. First hyperpolarizabilities β were obtained from EFISHG measurements which were performed on a Q-switch Nd:YAG laser emitting 6 ns pulses at 1064 nm (repetition rate: 10 Hz; typical energy per pulse: 100 mJ) and Raman shifted to 1907 nm with a high-pressure (50 bar) hydrogen cell. The EFISHG method has been described previously.[61]

SHG measurements on thin films were carried out using the same Nd:YAG laser at 1907 nm. The experimental setup has been described elsewhere.[62] In order to monitor the dynamics of SHG generation, SHG measurements have been made at a fixed incident angle (30°) during the poling cycle. The second-order susceptibilities d_{33} of the copolymer films have been determined at 1907 nm by the Maker fringe method. For

absolute determination of second-order susceptibilities d_{33}, a reference SHG signal was generated by using a Y-cut quartz crystal (3 mm thick, d_{11} = 0.5 pm/V at 1907 nm).

Temporal stability of dipole alignment was determined by monitoring the decay of the SHG signal as a function of temperature. For that purpose, the poled polymer film was mounted again on the stage used for in situ poling measurements. An incident angle of 30° was chosen for the fundamental beam at 1907 nm.

Results and Discussion

Material Preparation. The polymerizations for the preparation of the ThV and DR19 copolymers were conducted in *N,N*-dimethylacetamide (DMAc) in the presence of CsF at 22 °C with reaction times varying between 6 and 12 h. In this reaction, the feed ratio of the decafluorodiphenyl compound over the sum of the bisphenol and diol was kept at 2.01/2.00 to ensure a linear polymer main chain with high molecular weight. The molar ratio of the chromophore containing bisphenol or diol over 6F-BPA in the feed was controlled in order to obtain a polymer with desired chromophore content. CsF has been shown to efficiently activate bisphenols as well as the alkylene diols for the reaction with the decafluorodiphenyl compound. The polymerizations of DFPSO with 6F-BPA alone or with a mixture of 6F-BPA and ThV or di-ThV dye displayed similar reaction rates and were completed in 6−12 h to produce copolymers with high molecular weights.

The ThV copolymers were then converted to the TCVT polymers by reacting with tetracyanoethylene (TCNE) in DMF. A 100% conversion can be easily obtained for all the ThV polymers when the reaction was conducted at 50 °C in the presence of excess of TCNE.[63] Two side reactions have been found to accompany with this reaction: one is the 2 + 2 cyclic addition of the TCNE to the C=C in the ThV, and the other is the hydrolysis of TCNE when trace of water present in the solvent.[63] The former is a completely reversible reaction, and the cycloaddition product reverted completely to double bond at 50 °C. But this reaction reduced TCNE concentration in the reaction solution. Therefore, excess TCNE is necessary to maintain a high reaction speed and a high conversion rate. The latter is caused by trace water in the solvent to consume extra TCNE. Therefore, a carefully dried DMF is required for this reaction.

The chemical structures and compositions of the copolymers were verified by ^{1}H and ^{19}F NMR studies. The spectra of the copolymers before and after the reaction with TCNE were compared with a typical example shown in Figure 1 for the preparation of FPAES-TCVT-3. The spectra were recorded in DMSO-d_6. The peaks in the ^{1}H NMR spectra (Figure 1a) can be clearly assigned with the structure displayed in the figure. It showed that the reaction of the thiophene group in the polymer with TCNE led to a significant shift of the proton peaks of the thiophene group to high frequencies due to the very strong electron-withdrawing effect of the attached tricyanovinyl group.

The ^{19}F NMR spectra of the ThV polymer before and after the reaction with TCNE displayed a similar feature (Figure 1b). All the fluorine peaks had about 0.3 ppm shift to lower frequencies after the reaction, indicating the triphenylamine unit has lower electron density in TCVT. This is an evidence for the formation of intramolecular charge transfer (ICT) structure in the formed TCVT structure. On the other hand, the intensity of the peak of the fluorines adjacent to 6F-BPA and those adjacent to ThV kept the ratio of 2/1, indicating that the composition of the polymer is consistent

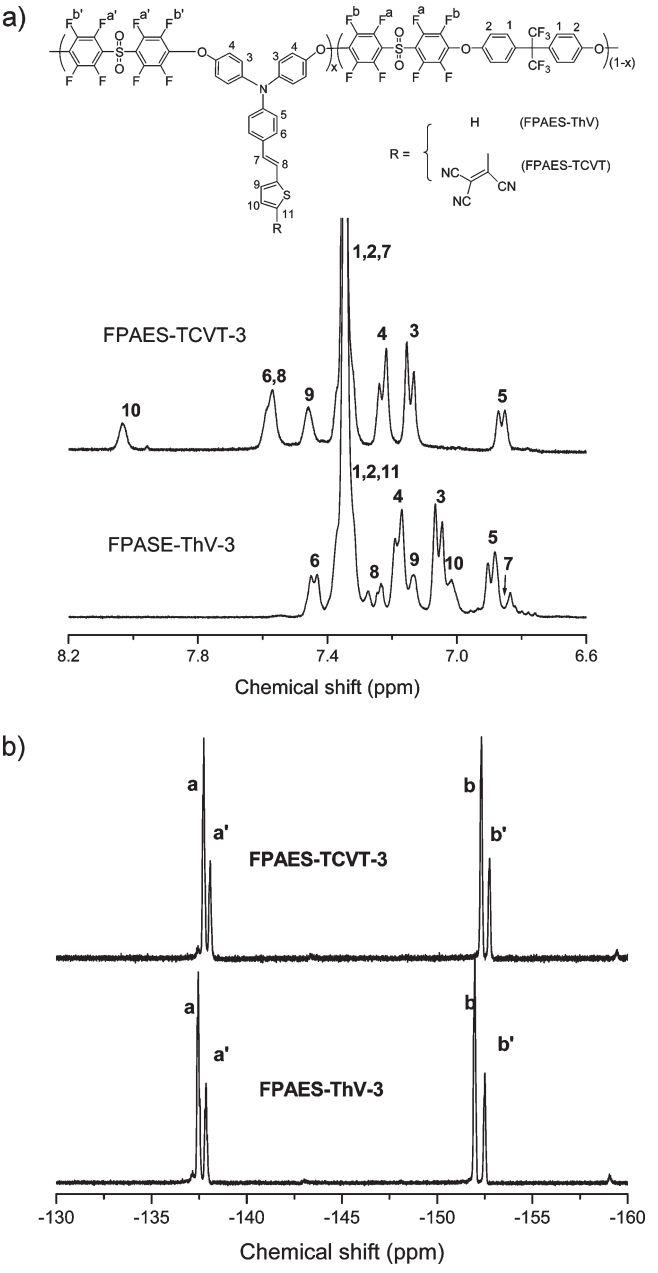

Figure 1. (a) Aromatic region of ^{1}H NMR spectra (in DMSO-d_6) of FPAES-ThV-3 and its product of the reaction with TCNE in DMF at 50 °C for 24 h. (b) Aromatic region of ^{19}F NMR spectra (in DMSO-d_6) of FPAES-ThV-3 and its product of the reaction with TCNE in DMF at 50 °C for 24 h.

with the feed ratio in the initial reaction mixture. This result also confirmed the completion of the postpolymerization reaction with TCNE.

The molecular weight and the molecular weight distribution of the polymers at different steps of the synthesis are summarized in Table 1. The homopolymers, ThV polymers, and DR19 polymers were prepared from the polycondensation of DFPSO with 6F-BPA and/or the chromophoric diol or bisphenol in the presence of CsF in DMAc at room temperature. They exhibited a high molecular weight and a wide molecular weight distribution (PDI). The wide PDI is related to the heterogeneous reaction conditions as explained in our previous paper.[57] The conversion of ThV polymer to TCVT polymer by reacting with TCNE in DMF at 50 °C only caused a slightly molecular weight reduction and had a

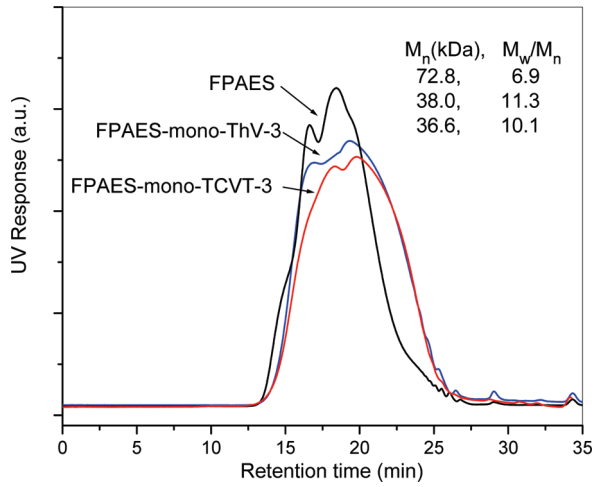

Figure 2. SEC curves of the polymers at different reaction stages for the preparation of FPAES-mono-TCVT-3.

negligible effect on the molecular weight distribution as demonstrated in Table 1 by comparing the M_n and PDI values of the ThV polymers with their corresponding TCVT polymers.

The preparation of FPAES-mono-TCVT-3 was started from a condensation reaction to attach the mono-ThV chromophore to homo-FPAES as a side group and then a reaction with TCNE to convert ThV to TCVT (see Scheme 5). The reaction to attach the mono-ThV chromophore onto the FPAES chain is conducted in the same reaction conditions as the polymerization leading to FPAES. It is designed to react the hydroxyl group of mono-ThV with the ortho-fluorines of the DFPSO unit to form an ether linkage with the ThV group pendulously attached. Usually, a conventional condensation reaction for the formation of ether bond is an equilibrium reaction. The addition of extra hydroxyl group into the polymer solution at the polymerization condition will lead to cleavage of the main chain ether bond. In this case, the mono-ThV possibly not only reacts with the ortho-fluorines on the DFPSO units but also potentially reacts with the ether group in the main chain. This side reaction will degrade the polymer and lead to a tremendous molecular weight decrease.[54] Fortunately, under the present reaction conditions, Figure 2 shows only a little change on the SEC curve after the reaction, while NMR study proved the successful attachment of mono-ThV to the polymer backbone. This result indicated that the ether cleaving side reaction is minor in this reaction, probably due to the extremely low reaction temperature. This is an encouraging result and is also an essential condition to use this reaction for the preparation of the FTC-type copolymers in this approach. Figure 2 also shows that the subsequent reaction of the obtained ThV polymer with TCNE did not result in an apparent molecular weight reduction, indicating the polymer is safe for the substitution with TCNE.

It is worth to note that the ^{19}F NMR spectrum of FPAES-DR19-3 displayed two sets of peaks in the regions between −136 and −139 ppm and between −151 and −156 ppm, corresponding to the fluorines on the DFPSO unit at the position ortho and meta to sulfone linkage. Each set contained four peaks with an intensity ratio of 9/3/3/1. They are attributed to the four triads with different combinations of the two adjacent units of DFPSO, DR19, and 6F-BPA. Using A to represent DR19 unit and B for 6F-BPA, the four combinations will be BB, BA, AB, and AA. Because the ratio of B/A is 3/1, the ratio of BB/BA/AB/AA will be (3 × 3)/(3 × 1)/(1 × 3)/(1 × 1) = 9/3/3/1. This result reflected that the polymer structure is perfectly consistent with the design. This phenomenon was also found in the ^{19}F NMR spectra of all the ketone polymers, DR19 polymers, FPAES-di-ThV, and FPAES-di-TCVT (see Experimental Section). A similar phenomenon was also reported for highly fluorinated aromatic−aliphatic copolyethers in one of our previous papers.[56]

Characterizations. The thermal properties of the polymers have been characterized by DSC and TGA with the results summarized in Table 1. It can be seen from the DSC measurements that all the polymers are amorphous materials, with no first-order transition found in the tested temperature range from −50 to 250 °C. The glass transition temperatures of all these polymers are high in the range between 150 and 215 °C. It is shown that the sulfone polymers have higher T_g than ketone polymers, and the T_g of the final TCVT polymers is higher than that of ThV polymers, attributed to the higher polarity of the TCVT unit than ThV. When the rigid phenyl tethers were replaced by flexible ethylene tethers, the T_g value was reduced. For example, the T_g of FPAES-ThV-3 polymer with phenyl tethers was 195 °C. This value was reduced to 164 °C in FPAES-di-ThV-3 polymer. Attaching the tricyanovinyl group to the end of the ThV unit increased the polarity of the polymers and therefore significantly increased the T_g values to 213 °C for FPAES-TCVT-3 and to 185 °C for FPAES-di-TCVT-3 (see Supporting Information).

The rigid FPAES and FPAEK homopolymers consist of symmetrical aromatic ethers. These polymers have higher thermal stability with a $T_d^{5\%}$ value higher than 450 °C (see Table 1). Introduction of ThV chromophore into the polymers did not apparently affect this value, indicating a very high thermal stability of the ThV chromophore unit in the polymers. After the ThV chromophore was converted to the TCVT, the $T_d^{5\%}$ value of the formed polymers only had a slight decrease of about 20 °C. But the TGA curve of these polymers displayed a much lower onset of the degradation with the $T_d^{1\%}$ value about 80 °C lower than ThV polymer. This result suggests that the TCVT polymers have a much lower thermal stability and start to degrade at about 350 °C, though the weight loss process is very slow. On the other hand, the polymers with asymmetrical ether linkage such as FPAES-di-TCVT and FPAES-di-ThV displayed a very fast degradation at much lower temperature, with the $T_d^{5\%}$ value of around 280 °C, which is about 170 °C lower than the polymers with symmetrical ether linkage. This value is extraordinarily low. Though a lower $T_d^{5\%}$ with ∼50 °C decrease was also found for the analogous asymmetric fluorinated aromatic−aliphatic polyethers compared with the symmetric fluorinated aromatic polyethers,[56] it is only about 1/3 of the reduction found for the present polymers. Therefore, the much lower thermal stability of the asymmetric copolymers in this work must be attributed to a synergistic effect by both asymmetric ether structure and the chromophore structures. It can be confirmed by a further investigation of the TGA curve of these polymers with an example shown in Figure 3 which revealed two decomposition steps. The weight loss of the first step corresponds to the loss of the chromophore units; the second step displayed a similar behavior as the homopolymers.

The synthesized copolymers were soluble in common solvents such as acetone, THF, chloroform, DMF, DMSO, and cyclohexanone. Among them, we found that cyclohexanone gave films with the best optical quality. The spin-casting of solutions of the highly fluorinated copolymers (6% w/w) in cyclohexanone at a speed of 500 rpm on clean

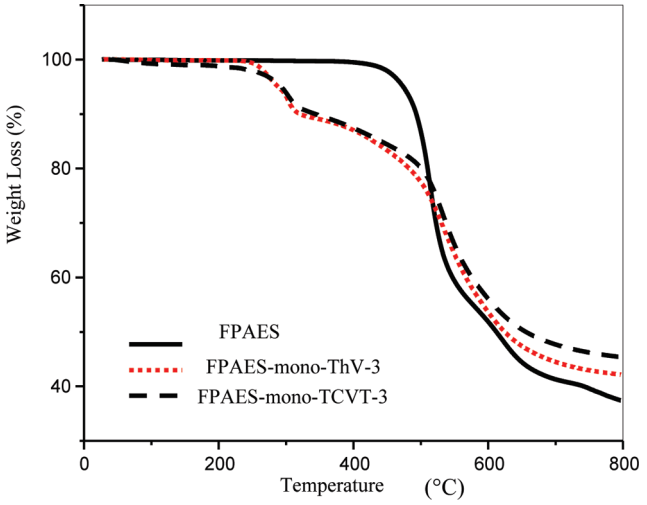

Figure 3. TGA curves of FPAES, FPAES-mono-ThV-3, and FPAES-mono-TCVT-3.

glass slides resulted in films with thicknesses around 500 nm. In all cases, the spin-coated polymer films were smooth on the surface and homogeneous in the film. The maximum absorption wavelengths of the copolymers which contained DR1 and DR19 chromophores were between 450 and 480 nm, while those for the other copolymers with the TCVT group were around 620 nm (see Figure 4). These data clearly indicate that the observed absorptions were due to the NLO chromophores since the backbone polymers (homo-FPAEK and homo-FPAES) films were almost transparent in the visible region. Moreover, the tricyanovinyl group, which is the strongest electron-withdrawing group, consequently inducing a larger charge transfer in the chromophore, gives copolymers with the largest bathochromic shift and with an absorption maximum near 620 nm. The absorption maxima of the films are nearby the absorption maxima of polymers dissolved in cyclohexanone (see Table1); the slight differences observed can be explained by a solvatochromic effect. Moreover, increasing the chromophore loading never led to a significant change in maximum. So we concluded that no aggregation occurred in the copolymer films under study.

The refractive indices of the copolymers were measured at 954 and 1907 nm with the values listed in Table 1. These values are necessary for the determination of the second-order susceptibilities of the poled films. They are slightly higher than those of the corresponding homopolymers (1.50 for homo-FPAEK and 1.51 for homo-FPAES at 1550 nm). This increase is due to the contribution of the NLO chromophores.

EFISHG Measurements of Chromophores. The $\mu\beta$ value of the model chromophore, TCVT, in chloroform solutions was obtained by the EFISHG technique, with the fundamental laser wavelength fixed at 1907 nm. Both this wavelength and the second harmonics wavelength (953 nm) are far off the resonance peak of the first electronic transition of the chromophores used in this paper. TCVT has a large $\mu\beta$ value ($\mu\beta_{1907} = 3750 \times 10^{-48}$ esu). Taking into account the absorption spectrum of TCVT in chloroform and applying the two-level model[64] allow estimating the zero-frequency $\mu\beta_0$ value, which is equal to 1960×10^{-48} esu. This value is comparable with that of 1-(4′-diethylaminophenylthienyl)-1,2,2- tricyanoethylene ($\mu\beta = 6200 \times 10^{-48}$ esu measured at 1907 nm, which leads to $\mu\beta_0 = 3023 \times 10^{-48}$ esu).[65] Assuming that the values of the ground-state dipole moments are similar for these two molecules, we conclude that substitution

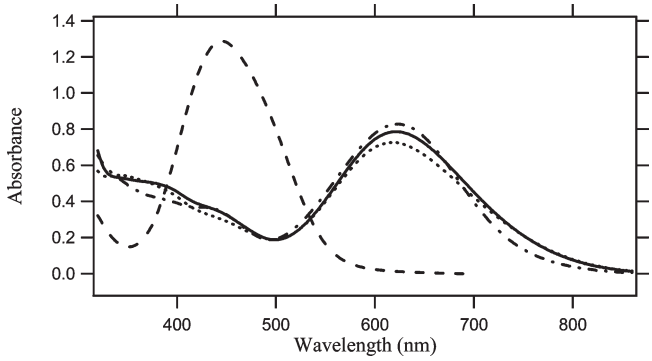

Figure 4. Absorption spectra of thin films of the following copolymers: PBA-TCVT-2 (dash-dot), FPAES-TCVT-3 (solid), FPAEK-TCVT-3 (dot), and FPAES-DR19-3 (dash).

of two ethyl groups by two phenol groups in TCVT leads to a decrease of 30% of the hyperpolarisability. The dipole moment of TCVT has been determined by the Guggenheim method and found equal to 8.9 D, which leads to $\beta_0 = 220 \times 10^{-30}$ esu. For sake of comparison, the β_0 value of DR1 was 50×10^{-30} esu.[66]

Second-Order Susceptibilities of the Copolymers. Inspection of the film surfaces by atomic force microscopy (AFM) showed that the roughness of the prepared films varied between 0.5 and 2 nm. After poling by the corona discharge, the AFM images as shown in Figure 5 display a dramatic change of the surface structure with small spikes appearing at a maximum height of 9 nm, indicating an increased surface roughness. Such a change of the surface morphology of the film after corona poling has been already observed, with almost the same peak heights.[25] The measurements of second-order susceptibilities have been performed after the optimization of the poling conditions. The maximum temperature used during the poling cycle which gives the best in situ SHG signal was around ($T_g - 20$) °C for all the studied copolymers.

The d_{33} values, measured for all the studied polymers 1 day after poling, increased in the same order as the β values of the chromophores and also increased with the molar ratio of the chromophores in the copolymers (Table 2). For comparison, a copolymer of methyl methacrylate with pendant DR1 groups (PMMA-DR1) was also studied under the same poling conditions. The films prepared from the copolymers PBA-TCVT-2 and FPAEK-TCVT-3 showed a better value of second-order susceptibility at 1907 nm compared to the copolymer of PMMA-DR1. However, the nonresonant value $d_{33}(0)$ is better for PMMA-DR1, in spite of a lower hyperpolarizability for DR1 compared to TCVT (4 times less). The origin of these values lower than expected will be discussed below after in situ monitoring of the SHG signal during poling.

The values of $d_{33}(0)$ obtained for the different highly fluorinated copolymers can only be compared with similar copolymers bearing similar chromophores linked in the same way to the main polymer chain. For example, in the domain of fluorinated polyarylene ethers, FPAES-DR1-6 ($d_{33}(0) = 5.6$ pm/V) can be compared with polymer P1 of ref 51 ($d_{33}(0) = 10$ pm/V) or polymer 6FBA-DR1 of ref 50 ($d_{33}(0) = 12$ pm/V). The mole fraction of the dye content is higher in these two examples. The same copolymer can also be compared with a non-fluorinated poly(arylene ether sulfone) (P1) of ref 67 with a chromophore similar to DR1 at a similar molar fraction ($d_{33}(0) = 6.6$ pm/V). There are few examples in the literature of copolymers with TCVT chromophore. For a polyurethane bearing TCVT chromophore linked to the

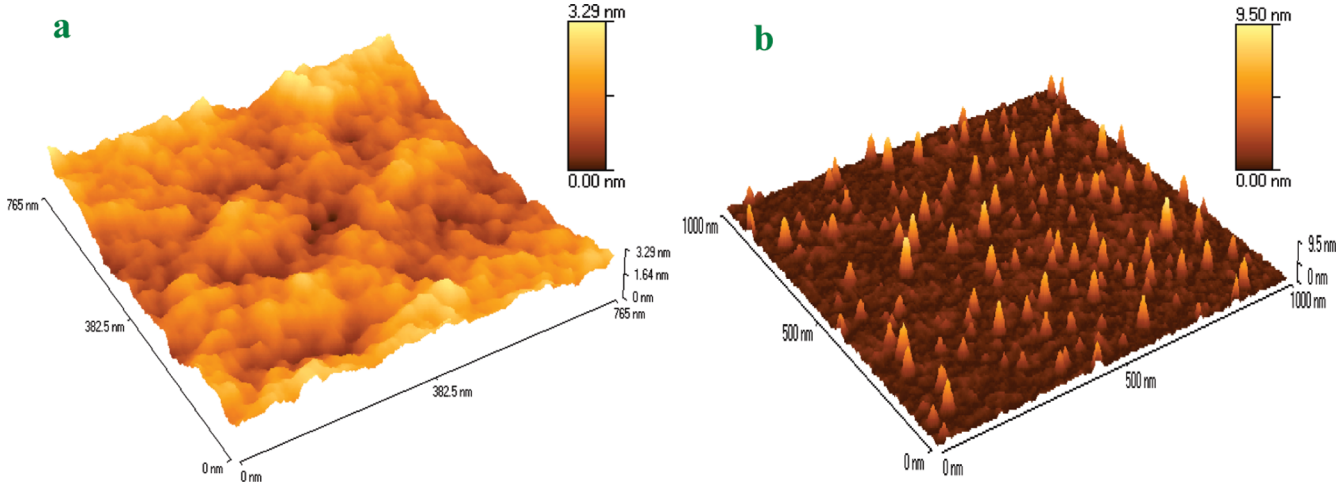

Figure 5. AFM images of the surface of the FPAEK-TCVT-1 film: (a) before corona poling; (b) after corona poling.

Table 2. Order Parameters and Second-Order Susceptibilities of the Different Fluorinated Copolymers Studied in This Work

copolymers	chromophore loading (%)	T_g (°C)	$T_{poling} \pm 5$ (°C)	order parameter Φ (%)[a]	d_{33}(1907) (pm/V)	d_{33}(0) (pm/V)
FPAES-DR19-3	25	178	160	17.1 ± 1.8	3	2
FPAES-DR19-5	50	171	155	13.1 ± 1.5	5	4
FPAES-TCVT-1	14	196	160	19.8 ± 2.4	6	3
FPAES-TCVT-3	33	213	180	20.1 ± 3.2	4	2
FPAEK-TCVT-1	14	168	160	32.3 ± 3.3	9	5
FPAEK-TCVT-3	33	187	170	22.2 ± 1.8	15	8
PBA-TCVT-2	23	182	170	38.4	15	8
FPAES-di-TCVT-3	33	185	170		8	4
FPAES-mono-TCVT-3	30	195	175		12	6
FPAES-DR1-6	64	174	160	15.2	8	6
PMMA-DR1	30	125	120	16.3	18	12

[a] $\Phi = 1 - A/A_0$, where A_0 and A are the maximum absorbance before and after poling.

main chain via two flexible links as FPAES-di-TCVT-3 ($d_{33}(0) = 3.8$ pm/V), a value of d_{33} of 51 pm/V at 1064 nm was obtained.[20b] This fundamental wavelength needs to rectify the determination of d_{33} for absorption and resonance, which unfortunately makes the comparison difficult.

During in situ monitoring of the SHG signal, we observed an unusual decay of the SHG signal of the FPAES-TCVT and FPAEK-TCVT copolymer films at the temperature below 130 °C during the cooling cycle, while the electric field was still applied. A SHG signal loss up to 70% (Figure 6, upper left curve) was observed. For the sake of comparison, we did the same in situ SHG measurements during poling PMMA-DR1 (Figure 6, upper right). Its SHG signal increased slightly at the beginning of the cooling period, and no decay was observed later, as far as the corona field was on. This increase can be explained by a competition between Brownian motion which decreases as temperature is lowered (and tends to make dipole orientation easier at low temperatures) and viscosity which decreases with temperature (and tends to impede poling at low temperatures). The drop in SHG during cooling observed for the fluorinated polymers seems typical of this kind of polymer and has never been described before. In order to be sure that it is due to disorientation of the dipoles, and not to some degradation of the polymer film, we perform in situ absorption measurements during poling (see Supporting Information), where we observed an usual decrease of absorbance during cooling, whereas followed by an increase when the temperature was lowered below 130 °C. This increase is due to a randomization of the previously oriented dipoles, which occurs in spite of the applied potential. This effect should be due to strong intrachain and/or interchain interactions implying the numerous dipoles of the chromophores and of the chains (carbonyl and sulfonyl groups, CF_3 groups, ether linkages). The interaction of the dipoles along one chain can be visualized by performing DFT simulation using Gaussian 03,[68] with a B3LYP/6-31G orbital basis.[69] One unit of the copolymer FPAEK-TCVT has been simulated to check the spatial orientation of the different dipoles in the space. This simulation shows that, in the lowest energy configuration, there are interactions between the different dipoles which orient themselves head to tail along the polymer chain (Figure 7). This orientation of the dipoles, facilitated by the dipole−dipole interaction, in addition to the rigidity of the linkage between the chromophore and the main chain in FPAES-TCVT and FPAEK-TCVT prevents an easy alignment of the chromophores under an applied external electric field.

When temperature cycles were applied to the film, the change of SHG signal was shown to be reversible and approximately occurred at the same temperature for different cycles (Figure 8). Surprisingly, the SHG signal increased much faster in the second and succeeding cycles than in the first one, indicating the orientation is much easier and faster for the sample which was previously poled. This phenomenon might imply that though a large fraction of the chromophores randomized during the cooling, owing to the strong dipolar interaction between the chromophores, the free volume created during the previous poling can be maintained a long period of time, which facilitates the poling in the second and succeeding temperature cycles.

Since the dipolar interactions as well as the tether between the chromophore and the main chain seem to play an important role in this relaxation process, we considered the

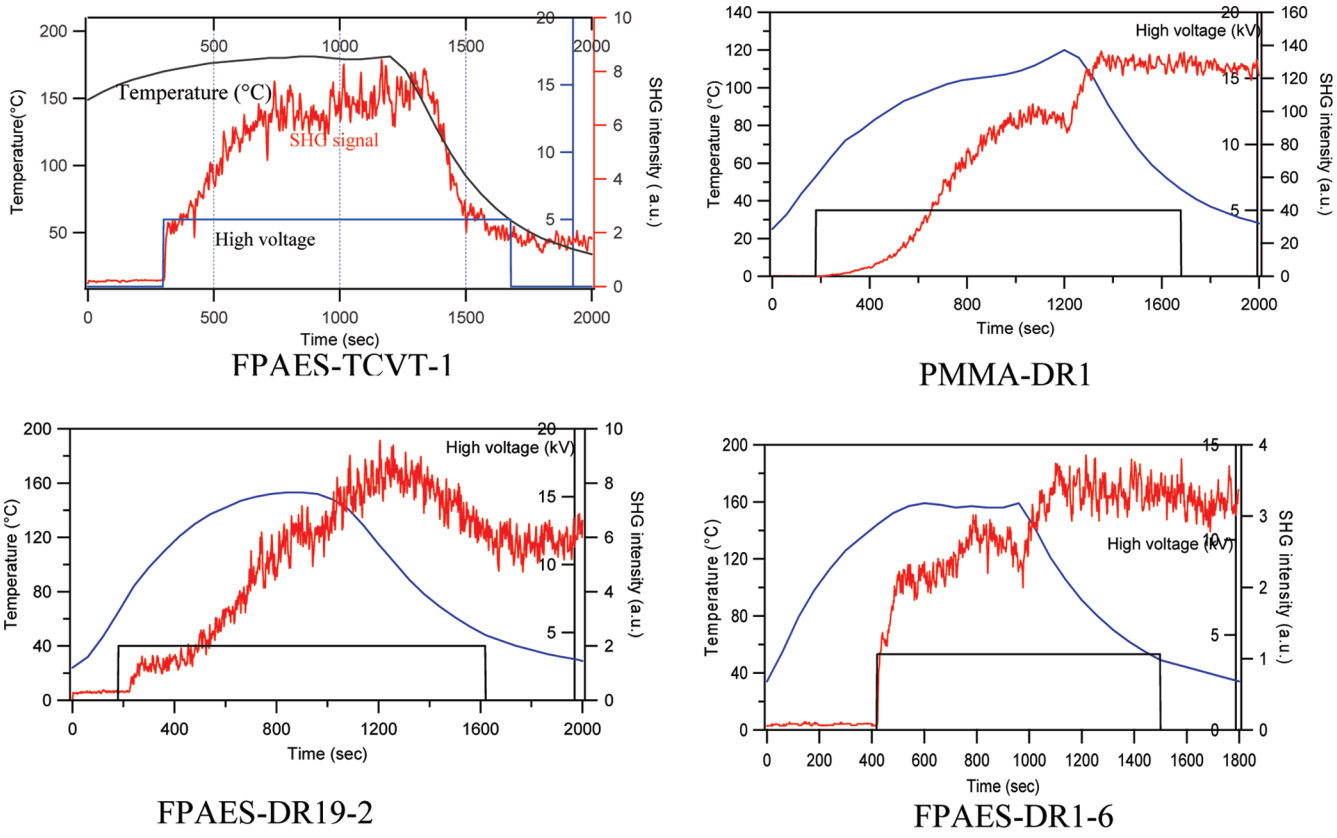

Figure 6. In situ SHG (measured at 1907 nm) of different highly fluorinated copolymer films compared with in situ SHG of PMMA-DR1 copolymer. The SHG intensities are given in arbitrary units.

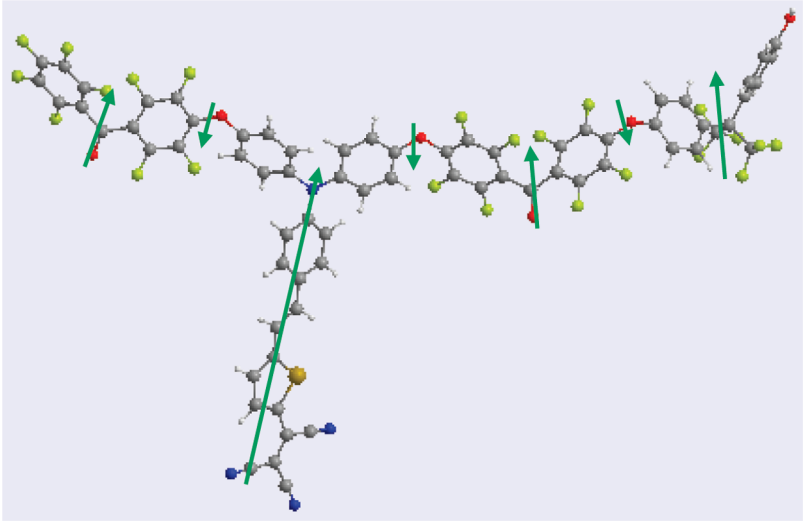

Figure 7. Optimized geometry of copolymer FPAEK-TCVT. The arrows show the dipole orientations.

influence of the polymer structures by varying, as shown in Scheme 1, the nature of the polar groups in the main chain, the nature of the chromophores, and also the type of tether between the chromophore and the main chain. The results are presented in Table 3 (see also Supporting Information). The conclusions of this extensive study are the following: (i) Replacement of the keto group by the sulfo group (and keeping the same chromophore TCVT) had no effect on the drop; furthermore, the elimination of these two polar groups in the polymers such as PBA-TCVT did not suppress the drop. (ii) The more rigid the tether between the chromophore and the chain, the larger the drop of SHG. In FPAES-di-TCVT, the chromophore is linked via two flexible alkyl chains, and the drop is lowered to 50%. This drop decreased to 30% for FPAES-mono-TCVT, where the chromophore was linked to main chain by only a single flexible tether. (iii) The larger the polarity of the chromophore, the larger the drop: DR19 and DR1 chromophores led to a lower drop than TCVT. Finally, there is almost no drop observed for FPAES-DR1-6 (see Figure 6). This copolymer behaved almost in the same manner as the reference polymer PMMA-DR1. Clearly, besides the nature of the chromophores,

Table 3. Relation between the Amplitude of the Drop of SHG Signal and the Structure of the Copolymers

				main structural parameters	
polymer	T_g[a] (°C)	T_{drop}[b] (°C)	SHG drop amplitude (%)	tether between chromophore and main chain	main chain
FPAES-TCVT-1	196	130 ± 10	70	DEMC (two rigid tethers)	dipoles in main chain
FPAES-TCVT-3	213	130 ± 10	75	DEMC (two rigid tethers)	dipoles in main chain
FPAEK-TCVT-1	168	130 ± 10	70	DEMC (two rigid tethers)	dipoles in main chain
FPAEK-TCVT-3	187	130 ± 10	70	DEMC (two rigid tethers)	dipoles in main chain
FPAES-DR19-3	178	110 ± 10	20	DEMC (two flexible tethers)	dipoles in main chain
FPAES-DR19-5	171	100 ± 10	30	DEMC (two flexible tethers)	dipoles in main chain
FPAES-di-TCVT-3	185	110 ± 10	50	DEMC (two flexible tethers)	dipoles in main chain
PBA-TCVT-2	182	120 ± 20	70	DEMC (two rigid tethers)	less dipoles in main chain
FPAES-DR1-6	174		< 5	FTC (one flexible tether)	dipoles in main chain
FPAES-mono-TCVT-3	195	100 ± 20	30[c]	FTC (one flexible tether)	dipoles in main chain

[a] T_g: glass transition temperature. [b] T_{drop}: temperature where the SHG signal starts decreasing. [c] For this polymer, the relaxation rate is slower than for the others.

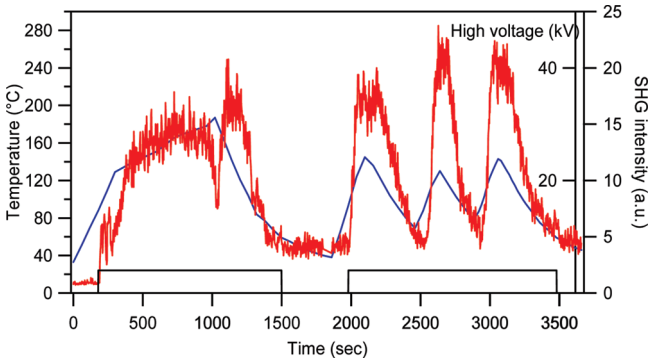

Figure 8. Several orientation cycles on a film of FPAES-TCVT-3 (T_g = 213 °C).

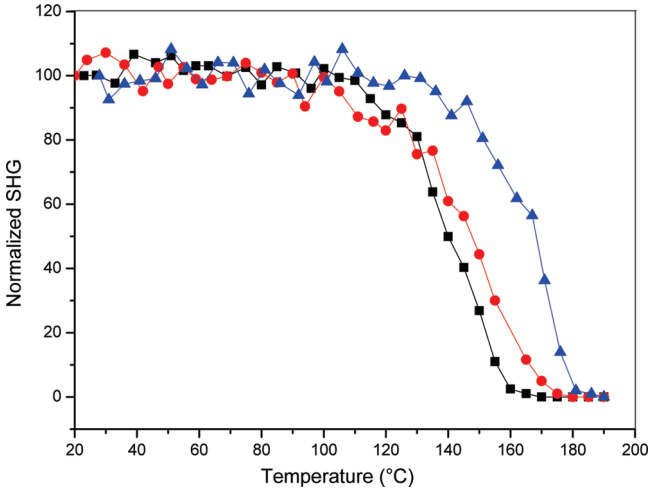

Figure 9. Thermal relaxation of the SHG signal of poled films of (■) FPAES-DR19-5 copolymer (T_g = 171 °C), (●) FPAEK-TCVT-1 copolymer (T_g = 168 °C), and (▲) PBA-TCVT-2 copolymer (T_g = 182 °C) with a heating rate of 5 °C/min from 30 to 190 °C.

which determines the strength of the dipolar interaction, the dominant factor seems to be the nature of the tether; a rigid tether seems to induce a transition to reduce polar order. Secondary glass transitions have been invoked to explain relaxation phenomena at temperatures lower than T_g: we already put evidence into this relaxation phenomenon in polyimides.[70] However, DSC measurements did not point out such a transition as there is no discontinuity in the DSC curves around 120 °C (see Supporting Information). More sensitive methods like dielectric measurements, which are able to put into evidence α, β, and δ transitions in copolymers,[71−73] are therefore in progress to put into evidence secondary glass transitions in these new materials. The tether between the NLO chromophore and the chain and the chromophore−chromophore interactions have been shown to play an important role in this relaxation. This consideration allowed to theoretically predict an optimal chromophore concentration.[74] But the influence of the mobility of the tether between the chromophore and the main chain together with the polarity of the main chain is still to be considered.

In order to evaluate the high-temperature stability of these poled copolymers, we studied the temporal stability of the SHG signal measured 1 day after poling. Figure 9 shows the SHG signal evolution with temperature for three different poled polymer films.

For all these copolymers, the SHG signal is quite stable up to 130 °C (at which the SHG signal decayed 10% of its initial value) and starts to decay at temperatures above 130 °C. This temperature is about 40 °C below the T_g of each copolymer and close to the temperature where a drop in the SHG signal intensity was observed previously during cooling (see above). But PBA−TCVT copolymer shows better stability until 150 °C. So, the decay onset of the SHG signal is lower than T_g for all these copolymers, as already observed for fluorinated poly(arylene ether)s.[50,51] The same conclusion also holds for several NLO polyimides,[12,13,49] with some counterexamples where the onset is nearby T_g[15] or much higher than T_g.[17] These experiments of thermal stability also point to a secondary glass transition which occurs in the temperature range between 100 and 130 °C and which is responsible for the loss of the dipole alignment during heating of the poled films above this temperature.

Conclusion

A new family of NLO-active highly fluorinated poly(arylene ether sulfone)s, poly(arylene ether ketone)s, and poly(arylene ether)s bearing chromophore derivatives of Disperse Red 1 or TCVT have been synthesized under mild conditions, fully characterized for both their physicochemical and optical properties. The glass transition temperatures are higher than 170 °C for all the copolymers studied. SHG measurements indicated nonresonant d_{33} values ranging from 2 to 8 pm/V, depending on both the nature and molar fraction of the chromophore. The SHG signals are thermally stable below 130 °C. The in situ monitoring of SHG signals during poling points out an important loss of the second-order activity during the cooling step under corona discharge. The extent of this loss has been correlated with the polymer structure and has put into evidence the predominant role of the tether between the chromophore and the main polymer chain, a flexible linkage leading to a much lower loss. This loss has been

attributed to a relaxation process involving interchain dipolar interaction between NLO chromophores. Further experiments involving dielectric measurements are in progress to put into evidence that this process is attributed to a secondary glass transition.

Acknowledgment. The authors thank Elena Ishow (PPSM, ENS Cachan) for helpful discussions in the synthesis of chromophores and Arnaud Brosseau (PPSM, ENS Cachan) for performing DSC measurements and Chi Thanh Nguyen (LPQM, ENS Cachan) for ellipsometric measurements.

Supporting Information Available: DSC curves, spectroscopic ellipsometry measurements, in situ absorption, and NLO measurements during poling. This material is available free of charge via the Internet at http://pubs.acs.org.

References and Notes

(1) Nalwa, H. S.; Watanabe, T.; Miyata, S. In *Nonlinear Optics of Organic Molecules and Polymers*; Nalwa, H. S., Miyata, S., Eds.; CRC Press: Boca Raton, FL, 1997; p 89.
(2) Jang, S.-H.; Jen, A. K.-Y. In *Introduction to Organic Electronic and Optoelectronic Materials and Devices*; Sun, S.-S., Dalton, L. R., Eds.; CRC Press: Boca Raton, FL, 2008; p 450.
(3) (a) Shi, Y.; Zhang, C.; Zhang, H.; Bechtel, J. H.; Dalton, L. R.; Robinson, B. H.; Steier, W. H. *Science* **2000**, *288*, 119. (b) Lee, M.; Katz, H. E.; Erben, C.; Gill, D. M.; Gopalan, P.; Heber, J. D.; McGee, D. J. *Science* **2002**, *298*, 1401. (c) Marder, S. R.; Kippelen, B.; Jen, A.K-Y.; Peyghambarian, N. *Nature* (*London*) **1997**, *388*, 845.
(4) Marks, T. J.; Ratner, M. A. *Angew. Chem., Int. Ed. Engl.* **1995**, *34*, 155.
(5) Burland, D. M.; Miller, R. D.; Walsh, C. A. *Chem. Rev.* **1994**, *94*, 31.
(6) (a) Dalton, L. R. *Adv. Polym. Sci.* **2002**, *158*, 1. (b) Kajzar, F.; Lee, K.-S.; Jen, A. K.-Y. *Adv. Polym. Sci.* **2003**, *161*, 1.
(7) (a) Zhang, C.; Wang, C.; Yang, J.; Dalton, L. R.; Sun, G.; Zhang, H.; Steier, W. H. *Macromolecules* **2001**, *34*, 235. (b) Zhang, C.; Wang, C.; Dalton, L. R.; Zhang, H.; Steier, W. H. *Macromolecules* **2001**, *34*, 253. (c) Ma, H.; Wu, J.; Herguth, P.; Chen, B.; Jen, A. K.-Y. *Chem. Mater.* **1999**, *11*, 452.
(8) Haller, M.; Luo, J.; Li, H.; Kim, T.-D.; Liao, Y.; Robinson, B. H.; Dalton, L. R.; Jen, A. K.-Y. *Macromolecules* **2004**, *37*, 688–690.
(9) Wu, J. W.; Valley, J. F.; Ermer, S.; Binkley, E. S.; Kenney, J. T.; Lipscomb, G. F.; Lytel, R. *Appl. Phys. Lett.* **1991**, *58*, 225–227.
(10) Stähelin, M.; Walsh, C. A.; Burland, D. M.; Miller, R. D.; Twieg, R. J.; Volksen, W. *J. Appl. Phys.* **1993**, *73*, 8471–8479.
(11) Becker, M. W.; Sapochak, L. S.; Ghosen, R.; Xu, C.; Dalton, L. R.; Shi, Y.; Steier, W. H.; Jen, A. K.-Y. *Chem. Mater.* **1994**, *6*, 104–106.
(12) Miller, R. D.; Burland, D. M.; Jurich, M.; Lee, V. Y.; Moylan, C. R.; Thackara, J. I.; Twieg, R. J.; Verbiest, R. J.; Volksen, W. *Macromolecules* **1995**, *28*, 4970–4974.
(13) Yu, D.; Gharavi, A.; Yu, L. *Macromolecules* **1996**, *29*, 6139–6142.
(14) Marestin, C.; Mercier, R.; Sillion, B.; Chauvin, J.; Nakatani, K.; Delaire, J. A. *Synth. Met.* **1996**, *81*, 143–146.
(15) Kim, T.- D.; Lee, K.-S.; Lee, G. U.; Kim, O.-K. *Polymer* **2000**, *41*, 5237–5245.
(16) Lu, J.-X.; Yin, J.; Deng, X. X.; Shen, Q.-S.; Cao-, Z.-Q. *Opt. Mater.* **2004**, *25*, 17–23.
(17) Lee, J.-Y.; Baek, C. S.; Park, E.-J. *Eur. Polym. J.* **2005**, *41*, 2107–2116.
(18) Wright, M. E.; Fallis, S.; Guenthner, A. J.; Baldwin, L. C. *Macromolecules* **2005**, *38*, 10014–10021.
(19) (a) Qiu, F.; Cao, Y.; Xu, H.; Jiang, Y.; Zhou, Y.; Liu, J. *Dyes Pigm.* **2007**, *75*, 454–459. (b) F.; Xu, H.; Cao, Y.; Jiang, Y.; Zhou, Y.; Liu, J.; Zhang, X. *Mater. Charact.* **2007**, *58*, 275–283.
(20) (a) Moon, K.-J.; Shim, H.-K.; Lee, K.-S.; Zieba, J.; Prasad, P. *Macromolecules* **1996**, *29*, 861–867. (b) Woo, H. Y.; Shim, H.-K.; Lee, K.-S. *Synth. Met.* **1999**, *101*, 136–137. (c) Apostoluk, A.; Nunzi, J.-M.; Lee, K.-S. *Opt. Commun.* **2006**, *263*, 337–341.
(21) Park, K. H.; Lim, J. T.; Song, S.; Lee, Y. S.; Lee, C. J.; Kim, N. *React. Funct. Polym.* **1999**, *40*, 177–184.
(22) Yuxia, Z.; Zhao, L.; Ling, Q.; Jianfen, Z.; Jiayun, Z.; Yuquan, S.; Gang, X.; Peixian, Y. *Eur. Polym. J.* **2001**, *37*, 445–449.
(23) Wang, C.; Zhang, C.; Lee, M. S.; Dalton, L. R.; Zhang, H.; Steier, W. H. *Macromolecules* **2001**, *34*, 2359–2363.
(24) Briers, D.; Picard, I.; Verbiest, T.; Persoons, A.; Samyn, C. *Polymer* **2004**, *45*, 19–24.
(25) (a) Lee, J.-Y.; Bang, H.-B.; Kang, T.-S.; Park, E.-J. *Eur. Polym. J.* **2004**, *40*, 1815–1822. (b) Lee, J.-Y.; Bang, H.-B.; Baek, C. S. *Synth. Met.* **2005**, *148*, 161–168. (c) Lee, J.-Y.; Baek, C. S.; Park, E.-J. *Eur. Polym. J.* **2005**, *41*, 2107–2116.
(26) Yang, Z.; Qin, A.; Zhang, S.; Ye, C. *Eur. Polym. J.* **2004**, *40*, 1981–1986. (b) Zhu, Z.; Li, Q.; Zeng, Q.; Li, Z.; Li, Z.; Qin, J.; Ye, C. *Dyes Pigm.* **2008**, *78*, 199–206.
(27) Caruso, U.; Casalboni, M.; Fort, A.; Fusco, M.; Panunzi, B.; Quatela, A.; Roviello, A.; Sarcinelli, F. *Opt. Mater.* **2005**, *27*, 1800–1810.
(28) Faccini, M.; Balakrishnan, M.; Diemeer, M. B. J.; Torosantucci, R.; Driessen, A.; Reinhoudt, D. N.; Verboom, W. *J. Mater. Chem.* **2008**, *18*, 5293–5300. (b) Faccini, M.; Balakrishnan, M.; Torosantucci, R.; Driessen, A.; Reinhoudt, D. N.; Verboom, W. *Macromolecules* **2008**, *41*, 8320–8323.
(29) Ma, H.; Wang, X.; Wu, X.; Liu, S.; Jen, A. K.-Y. *Macromolecules* **1998**, *31*, 4049–4052.
(30) Gubbelmans, E.; Verbiest, T.; Picard, I.; Persoons, A.; Samyn, C. *Polymer* **2005**, *46*, 1784–1795.
(31) Kim, T.-D.; Luo, J.; Cheng, Y.-J.; Shi, Z.; Hau, S.; Jang, S.-H.; Zhou, X.-H.; Tian, Y.; Polishak, B.; Huang, S.; Ma, H.; Dalton, L. R.; Jen, A. K.-Y. *J. Phys. Chem. C* **2008**, *112*, 8091–8098.
(32) Liao, Y.; Anderson, C. A.; Sullivan, P. A.; Akelaitis, A. J. P.; Robinson, B. H.; Dalton, L. R. *Chem. Mater.* **2006**, *18*, 1062–1067.
(33) (a) Blythe, A.; Vinson, J. *Polym. Adv. Technol.* **2000**, *11*, 601–611. (b) Zyss, J. *C. R. Phys.* **2002**, *3*, 403–405.
(34) Zhou, M. *Opt. Eng.* **2002**, *41*, 1631–1643.
(35) Groh, W. *Makromol. Chem.* **1988**, *189*, 2861–2874.
(36) Guyot, B.; Ameduri, B.; Boutevin, B.; Sideris, A. *Macromol. Chem. Phys.* **1995**, *196*, 1875–1886.
(37) Eldada, L.; Shacklette, L. *IEEE J. Quantum Electron.* **2000**, *6*, 54–68.
(38) Liang, J.; Toussaere, E.; Hierle, R.; Levenson, R.; Zyss, J.; Ochs, A. V.; Rousseau, A.; Boutevin, B. *Opt. Mater.* **1998**, *9*, 230–235.
(39) Pitois, C.; Vukmirovic, S.; Hult, A.; Wiesmann, D.; Robertsson, M. *Macromolecules* **1999**, *32*, 2903–2909.
(40) Onah, E. J. *Chem. Mater.* **2003**, *15*, 4104–4112.
(41) Jöhnck, M.; Müller, L.; Neyer, A.; Hofstraat, J. W. *Eur. Polym. J.* **2000**, *36*, 1251–1264.
(42) Kang, S. H.; Luo, J.; Ma, H.; Barto, R.; Frank, C. W.; Dalton, L. R.; Jen, A. K.-Y. *Macromolecules* **2003**, *36*, 4355–4359.
(43) Smith, D. W.; Babb, D. A. *Macromolecules* **1996**, *29*, 852–860.
(44) Kim, J.-P.; Lee, W.-Y.; Kang, J.-W.; Kwon, S.-K.; Kim, J.-J.; Lee, J.-S. *Macromolecules* **2001**, *34*, 7817–7821.
(45) Wong, S.; Ma, H.; Jen, A. K.-Y.; Barto, R.; Frank, C. W. *Macromolecules* **2003**, *36*, 8001–8007.
(46) Huang, W. Y.; Liaw, B. R.; Chang, M. Y.; Han, Y. K.; Huang, P. T. *Macromolecules* **2007**, *40*, 8649–8657.
(47) (a) Song, Y.; Wang, J.; Li, G.; Sun, Q.; Jian, X.; Teng, J.; Zhang, H. *Polymer* **2008**, *49*, 724–731. (b) Song, Y.; Li, G.; Wang, J.; Sun, Q.; Jian, X.; Teng, J.; Zhang, H. *Polym. J.* **2008**, *40*, 92–93. (c) Song, Y.; Wang, J.; Li, G.; Sun, Q.; Jian, X.; Teng, J.; Zhang, H. *Polymer* **2008**, *49*, 4995–5001.
(48) Ando, S.; Matsuura, T.; Sasaki, S. *Macromolecules* **1992**, *25*, 5858–5860.
(49) Bes, L.; Rousseau, A.; Boutevin, B.; Mercier, R.; Toussaere, E.; Zyss, J. *J. Opt. A: Pure Appl. Opt.* **2002**, *4*, 261–266.
(50) Ushiwata, T.; Okamoto, E.; Komatsu, K.; Kaino, T.; Jen, A. K.-Y. *Opt. Mater.* **2002**, *21*, 61–65.
(51) Lu, Z.; Shao, P.; Li, J.; Hua, J.; Qin, J.; Qin, A.; Ye, C. *Macromolecules* **2004**, *37*, 7089–7096.
(52) Chen, X.; Zhang, J.; Zhang, H.; Jiang, Z.; Shi, G.; LI, Y.; Song, Y. *Dyes Pigm.* **2008**, *77*, 223–228.
(53) Ding, J.; Liu, F.; Li, M.; Day, M.; Zhou, M. *J. Polym. Sci., Part A: Polym. Chem.* **2002**, *40*, 4205–4216.
(54) Ding, J.; Day, M.; Robertson, G. P.; Roovers, J. *Macromol. Chem. Phys.* **2004**, *205*, 1070–1079.
(55) (a) Qi, Y.; Ding, J.; Day, M.; Jiang, J.; Callender, C. L. *Chem. Mater.* **2005**, *17*, 676–682. (b) Ding, J.; Qi, Y.; Day, M.; Jiang, J.; Callender, C. L. *Macromol. Chem. Phys.* **2005**, *206*, 2396–2407. (c) Qi, Y.; Ding, J.; Day, M.; Jiang, J.; Callender, C. L. *Polymer* **2006**, *47*, 8263–8271.
(56) Ding, J.; Jiang, J.; Blanchetiere, C.; Callender, C. L. *Macromolecules* **2008**, *41*, 758–763.

(57) Ding, J.; Du, X.; Day, M.; Jiang, J.; Callender, C. L.; Stupak, J. *Macromolecules* **2007**, *40*, 3145–3153.
(58) Ding, J.; Qi, Y. *Macromolecules* **2008**, *41*, 751–757.
(59) Aljoumaa, K.; Ishow, E.; Ding, J.; Qi, Y.; Day, M.; Delaire, J. A. *Nonlinear Opt., Quantum Opt*. **2006**, *35*, 98–105.
(60) Nagtegaele, P. PhD Dissertation, Ecole Normale Superieure de Cachan, France, 2005.
(61) Janowska, I.; Zakrzewski, J.; Nakatani, K.; Delaire, J. A.; Palusiak, M.; Walak, M.; Scholl, H. *J. Organomet. Chem*. **2003**, *675*, 35–41.
(62) Averseng, F.; Lacroix, P. G.; Malfant, I.; Lenoble, G.; Cassoux, P.; Nakatani, K.; Maltey-Fanton, I.; Delaire, J. A. *Chem. Mater*. **1999**, *11*, 995–1002.
(63) Ding, J.; Robertson, G. P.; Lu, J. *Tetrahedron Lett*. **2008**, *49*, 3549–3553.
(64) Oudar, J. L.; Chemla, D. *J. Chem. Phys*. **1977**, *66*, 2664.
(65) Rao, V. P.; Jen, A.K.-Y.; Wong, K. Y.; Drost, K. J. *J. Chem. Soc., Chem. Commun*. **1993**, *14*, 1118–1120.
(66) Twieg, R.; Lee, V.; Miller, R. D.; Moylan, C.; Prime, R. B.; Chiou, G. *Polym. Prepr*. **1994**, *35*, 200.
(67) Lu, Z.; Li, J.; Hua, J.; Li, X.; Qin, J.; Qin, A.; Ye, C. *Synth. Met*. **2005**, *152*, 217–220.
(68) Frisch, M. J.; Trucks, G. W.; Schlegel, H. B.; Scuseria, G. E.; Robb, M. A.; Cheeseman, J. R.; Montgomery, Jr., J. A.; Vreven, T.; Kudin, K. N.; Burant, J. C.; Millam, J. M.; Iyengar, S. S.; Tomasi, J.; Barone, V.; Mennucci, B.; Cossi, M.; Scalmani, G.; Rega, N.; Petersson, G. A.; Nakatsuji, H.; Hada, M.; Ehara, M.; Toyota, K.; Dannenberg, J. J.; Zakrzewski, V. G.; Dapprich, S.; Daniels, A. D.; Strain, M. C.; Farkas, O.; Malick, D. K.; Rabuck, A. D.; Raghavachari, K.; Foresman, J. B.; Ortiz, J. V.; Cui, Q.; Baboul, A. G.; Clifford, S.; Cioslowski, J.; Stefanov, B. B.; Liu, G.; Liashenko, A.; Piskorz, P.; Komaromi, I.; Martin, R. L.; Fox, D. J.; Keith, T.; Al-Laham, M. A.; Peng, C. Y.; Nanayakkara, A.; Challacombe, M.; Gill, P. M. W.; Johnson, B.; Chen, W.; Wong, M. W.; Gonzalez, C.; Pople, J. A. *Gaussian 03*, Revision B.05; Gaussian, Inc.: Pittsburgh, PA, **2003**.
(69) Becke, A. D. *J. Chem. Phys*. **1993**, *98*, 564. (b) Lee, C.; Yang, W.; Parr, R. G. *Phys. Rev. B* **1988**, *37*, 785.
(70) Chauvin, J.; Nakatani, K.; Delaire, J. A.; Faure, S.; Mercier, R.; Sillion, B. *Synth. Met*. **2000**, *7432*, 1–6.
(71) Diaz-Calleja, R.; Riande, E. *Mater. Sci. Eng. A* **2004**, *370*, 21–33.
(72) Nikonorova, N. A.; Yakimansky, A. V.; Smirnov, N. N.; Kudryatsev, V. V.; Diaz-Calleja, R.; Pissis, P. *Polymer* **2007**, *48*, 556–563.
(73) Okutan, M.; Sentürk, E. *J. Non-Cryst. Solids* **2008**, *354*, 1526–1530.
(74) Pereverzev, Y. V.; Prezhdo, O. V.; Dalton, L. R. *ChemPhysChem* **2004**, *5*, 1821–1830.